Continual Learning in Human Activity Recognition: an Empirical Analysis of Regularization

Saurav Jha [1] **Martin Schiemer** [1] **Juan Ye** [1]

Abstract

Given the growing trend of continual learning techniques for deep neural networks focusing on the domain of computer vision, there is a need to identify which of these generalizes well to other tasks such as human activity recognition (HAR). As recent methods have mostly been composed of loss regularization terms and memory replay, we provide a constituent-wise analysis of some prominent task-incremental learning techniques employing these on HAR datasets. We find that most regularization approaches lack substantial effect and provide an intuition of when they fail. Thus, we make the case that the development of continual learning algorithms should be motivated by rather diverse task domains.

1. Introduction

The field of continuous learning for neural networks tries to develop algorithms that mimic the mammalian ability to incrementally learn new experiences without deterioration of older ones. Sensor-based human activity recognition (HAR) aims to autonomously categorize human activities using a range of sensors such as binary and proximity sensors, accelerometers, etc. to gather information about changes of state or physical activities. The use cases are manifold, ranging from smart homes (Zhang et al., 2020) to disease diagnosis (Afonso et al., 2019). HAR's potential benefits from *continuous* learning (often referred to as *lifelong/incremental* learning) are obvious: humans dynamically change their behavior and even develop new activities. Hence, algorithms must adapt to such ever changing diverse behaviors to prevent service quality degradation (Ye et al., 2019). One of the main stepping stones for continuous learning is that learning a new task interferes with previously acquired knowledge - a phenomenon known as *catastrophic forgetting* (CF) (McCloskey & Cohen, 1989). In general, we would prefer that models are *stable* enough to retain knowledge while being *plastic* enough to incorporate new information (Mermillod et al., 2013). In this paper, we address techniques that try to alleviate CF through regularization.

Algorithms leveraging regularization attempt to alleviate forgetting through the restriction of updates on network parameters. A substantial amount of these have achieved significant progress on image datasets, it is important to verify their generalization capabilities to other domains such as HAR which is marked by: (i) *dataset imbalance* – frequencies of activities can vary a lot with some being recurring while others rare; (2) *inter-class similarity* – activities might resemble each other thus forming overlapping inter-class boundaries; (3) *intra-class diversity* – an activity can be performed in different ways; and (4) *resource constraints* – most HAR systems are deployed on memory and computation-constrained devices such as wearables. Characteristics of the sensor datasets used, can be found in Appendices B and C.

The main contribution of our work lies in assessing the applicability and pitfalls of notable continual learning techniques on HAR[1]. Even though a high volume of continual learning techniques have been proposed in recent years, we focus on regularization and memory replay (MemR) techniques. We are not considering dynamic architecture approaches as HAR systems might not get to see a large number of classes (e.g., around 10-30).

We select five regularization-based methods, which range from classic methods such as LwF (Li & Hoiem, 2016) and EWC (Kirkpatrick et al., 2016), to more recent methods such as MAS (Aljundi et al., 2018), LUCIR (Hou et al., 2019) and ILOS (He et al., 2020). We assess these techniques on two third-party, publicly available datasets that are representative in two common sensor families: *accelerometer* and *ambient sensors*. Through an empirical evaluation on these datasets, we conclude that the regularization terms often have little or even detrimental effect in our scenarios (esp. together

[1] School of Computer Science, University of St Andrews, St Andrews, Scotland. Correspondence to: Saurav Jha <sj84@st-andrews.ac.uk>, Martin Schiemer <ms400@st-andrews.ac.uk>.

Proceedings of the 37^{th} International Conference on Machine Learning, Vienna, Austria, PMLR 119, 2020. Copyright 2020 by the author(s).

[1] Code will be made available at `https://github.com/srvCodes/continual-learning-benchmark`.

with memory replay) and may sometimes be worse than the lower boundary of applying plain cross-entropy (CE) loss.

2. Techniques

This section will briefly introduce the regularization terms whose description can be found in Appendix A. *LwF* employs knowledge-distillation (KD) loss (Hinton et al., 2015) to continuous learning with an objective of maintaining the logits of an incremental step model similar to its predecessor. *EWC* approximates the posterior distribution of network parameters and uses it to identify their importance and penalize their updates. Rotated EWC (RWC) (Liu et al., 2018) improves upon EWC by addressing its assumption that fisher information matrix in the network's parameter space are diagonal. Since this is often not the case, they rotate the parameter space in a manner that it does not alter the feed-forward response of the network. *MAS* calculates the importance of parameters by approximating the change in the network output caused by perturbations in parameters due to training on the new task data. *LUCIR* introduces two loss terms: *less forget constraint* (DIS) and *margin ranking* (MR)[2] with the goals of preventing rotation of old class embeddings and reducing ambiguities between old and new classes. *ILOS* modifies the CE loss by replacing the new model's logits for old classes with those adjusted proportionately between new and previous model. They coin the resultant loss as cross-distillation loss. We also consider lower bound as the model trained with CE loss and upper bound as the offline training with all tasks at the same time. The CE loss is defined as $\mathcal{L}_{CE}(y, \hat{y}) = -\sum y \log \hat{y}$, where y and and $\hat{y}$ are the ground truth and output logits for an input sample.

3. Experimental Setup

Our main objective is to assess which type of regularization term is effective for continual learning on sensor-based HAR and to what degree.

3.1. Datasets

We select two datasets from the sensor-based HAR community. The first dataset **(WS)** was collected on 32 ambient passive infra-red sensors by a smart home testbed at the Washington State University's CASAS.[3] It includes 9 imbalanced activities: cooking, eating, leaving/entering the house, living room activity, toilet use, mirror, reading, sleeping, and working. The second dataset is **DSADS** – Daily and Sports Activities Dataset (Altun & Barshan, 2010). It is a balanced dataset with 19 activities that include sitting, running on a treadmill, exercising on a stepper, and rowing among others - each of which is performed by 8 subjects for 5 minutes with 5 accelerometer units on a subject's torso, right arm, left arm, right leg and left leg. Circumventing the topic of feature extraction, we work on the features already extracted by prior work instead of the raw spatio-temporal sensor data. For DSADS, we use a version processed by Wang et al. (2018) which extracts 27 features (including mean, standard deviation, and correlations on axes) on each sensor. For WS, we use those generated by Fang et al. (2020).

3.2. Evaluation Process

Considering task order-sensitivity in continual learning paradigms (Yoon et al., 2019), we evaluate the techniques on 30 task sequences while updating the parameters on every incoming task. Each task is coupled with two randomly sampled classes, thus contributing to a sequence length of $|C|/2$, where $|C|$ is the total number of classes in the dataset.

We perform a stratified train-test split of 70/30 on WS dataset while for DSADS, we split data on participants; *i.e.,* we use data from 70% of subjects for training and the remaining 30% for testing. After training, we retain $\frac{S*|C|}{|C|_{seen}}$ random samples per class in the memory to be replayed at further incremental training steps. S is determined by the memory constraint of the HAR system and $|C|_{seen}$ is the number of classes observed till the current incremental step.

3.3. Evaluation Metrics

Upon arrival of a new task k, we compute four types of accuracy: *base* and *old* class accuracies measure performance on the very first (0^{th}) task and the tasks $\{1, .., k-1\}$ henceforth, thus indicating the *stability* of the model; *new* accuracy measures the performance on the current task thus indicating the *plasticity* of the model; and *overall* accuracy considers all the tasks learned so far, and implies the *stability-plasticity* balance of the model. The accuracy is measured in micro-F1 scores. Given the imbalanced class distribution in a real-world HAR scenario (see Appendix C), we additionally report macro-F1 scores.

For discerning the preservation of existing knowledge, we calculate the *forgetting measure* proposed by Chaudhry et al. (2018) which for task k is the difference between its maximum accuracy seen so far and the current accuracy averaged over $\{1, .., k-1\}$ tasks: $F_k = \frac{1}{k-1} \sum_{j=1}^{k-1} a_{k,j,max} - a_{k,j}$.

3.4. Model Configuration and Hyperparameter Tuning

Irrespective of their original works, we maintain a common network architecture across all our experiments as a fair comparison premise. We use fully-connected feed-forward networks with the following specifications optimized through extensive grid search: (1) DSADS: 3 hidden

[2] MR only applies to memory replay since in-memory samples are used to distance class embeddings.

[3] http://ailab.wsu.edu/casas/datasets/

Table 1. Performance comparison of different regularization terms. *wo.* and *w.* refer to *without* and *with* memory replay respectively.

Regularisation	WS				DSADS			
	wo. memory replay		w. memory replay		wo. memory replay		w. memory replay	
	micro-F1	macro-F1	micro-F1	macro-F1	micro-F1	macro-F1	micro-F1	macro-F1
CE (lower)	09.90 +/- 7.66	1.91 +/- 1.38	85.39 +/- 3.66	76.73 +/- 3.36	5.44 +/- 0.95	0.60 +/- 0.42	63.77 +/- 4.22	62.42 +/- 4.49
LwF	10.44 +/- 7.59	2.38 +/- 2.26	**86.89 +/- 4.36**	**77.16 +/- 5.49**	5.77 +/- 1.49	0.76 +/- 0.65	59.44 +/- 4.48	57.15 +/- 4.84
R-EWC	13.16 +/- 9.94	4.09 +/- 4.08	84.01 +/- 4.87	75.37 +/- 4.77	5.68 +/- 1.34	0.75 +/- 0.68	57.46 +/- 7.23	55.91 +/- 7.53
MAS	10.40 +/- 7.61	2.46 +/- 2.41	84.79 +/- 5.44	76.31 +/- 5.09	5.70 +/- 1.39	0.72 +/- 0.60	63.49 +/- 4.18	62.23 +/- 4.16
LUCIR-DIS	10.21 +/- 7.38	2.22 +/- 1.50	85.25 +/- 4.54	76.86 +/- 4.56	5.26 +/- 0.00	0.53 +/- 0.00	63.81 +/- 3.97	62.46 +/- 4.07
LUCIR-MR	-	-	86.00 +/- 4.66	77.12 +/- 4.12	-	-	71.29 +/- 2.84	70.05 +/- 2.95
LUCIR-DIS+MR	-	-	83.83 +/- 5.08	75.99 +/- 4.69	-	-	**71.69 +/- 2.39**	**70.54 +/- 2.74**
ILOS	**15.74 +/- 9.57**	**6.22 +/- 5.67**	83.02 +/- 7.07	73.12 +/- 6.00	**7.31 +/- 2.75**	**1.53 +/- 1.47**	61.14 +/- 3.68	59.42 +/- 3.78
OFFLINE (upper)	94.14	87.41	94.14	87.41	82.06	81.70	82.06	81.70

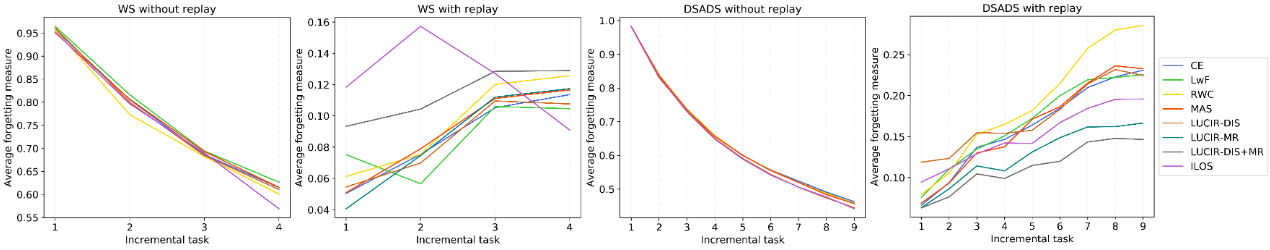

Figure 1. Forgetting measure comparison of losses with and without memory replay.

layers of sizes [202, 202, 101], and (2) WS: 2 hidden layers of sizes [32, 16, 16]. Each network has a single output head that gets extended on each incoming task to accommodate for new classes.

We perform a further search for technique-specific hyperparameters, detailed in Appendix D. It is worth noting that our LUCIR-based losses employ L2 normalization of the output logits of FC layer rather than the cosine normalization which offers a significant boost to performance in the original work of Hou et al. (2019). This compliments our fair premise assumption of assessing regularization alone.

4. Results

Fixed holdout size: Table 1 compares the micro and macro-F1 scores of regularization terms on WS and DSADS with and without MemR. The replay-based scores use $S = 6$ which we assume to be small enough to be held in a resource-constrained device and large enough to deliver decent performance. We find that most of the regularization techniques when devoid of replay only achieve the naive accuracy of baseline CE. In this scenario, ILOS with a direct influence of logits from the old model performs better than the rest where the models learn to align them as training progresses. When aided with replay, we find that CE alone beats most of the other techniques on both the datasets. For example, the improvements over the baseline CE approach remain within 1% on the WS dataset and within 8% on the DSADS dataset on both micro and macro-F1. We further observe that LUCIR's less-forget-constraint (DIS) does not provide a strong effect.

In terms of *task order-sensitivity* without MemR, LUCIR-DIS with the least average standard deviation has a clear win over the rest of the methods while ILOS and RWC offer less robustness. When MemR is used, the picture is more diverse between datasets as LwF and LUCIR-DIS+MR are the most stable for WS and DADS respectively.

We see that the differences between the F1 micro and macro scores vary across the methods. For the results without MemR, the micro scores are multiple times higher with CE being the most divergent (518% and 907%) while ILOS the least (253% and 448%). Table 3 in Appendix E presents the divergence scores between F1-micro and macro. From this, we conclude that the regularization methods help in learning fairer distributions of classes. In contrast, the advantage of the regularization methods with MemR is less apparent with no big difference to CE.

Forgetting: Figure 1 depicts the stark contrast of forgetting scores (F) of replay-assisted techniques to those without replay. Without MemR, F decreases sharply below 1.0 across all methods as the learning progresses beyond task 1. Although the strikingly high forgetting scores stipulate catastrophic forgetting on earlier tasks, these further shed light into the *stability* of techniques that are devoid of replay as their forgetting diminish with the arrival of further diverse tasks. On the other hand, the contribution of the regularization terms improve from being null to modest with MemR. In particular, we observe a threshold number of incremental tasks for replay-assisted methods following which the inertia of forgetting dampens. ILOS, LUCIR-MR and LUCIR-DIS+MR attain this threshold much earlier than CE. The high forgetting scores of RWC conform to the finding of Kemker et al. (2018) stating EWC-based methods are poor

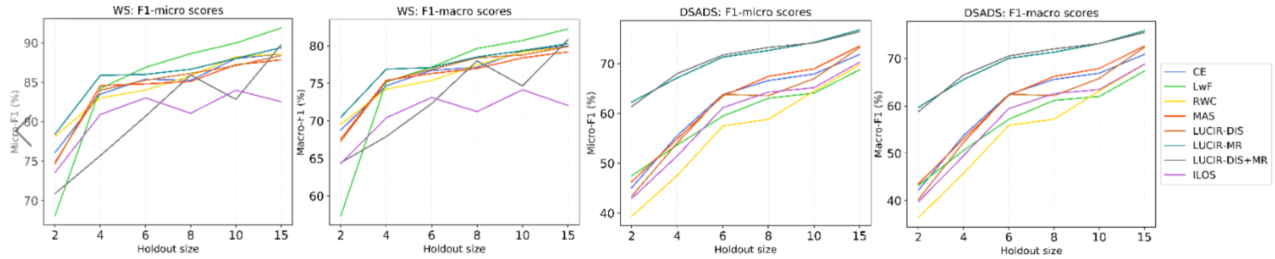

Figure 2. F1 performance comparison of different in-memory sizes. WS F1 scores on the left, DSADS on the right.

at learning new categories incrementally. LwF and ILOS start with relatively larger forgetting scores whose slope alleviates with further incremental steps. In contrast, margin ranking-based techniques have lesser overall forgetting scores, which accords with greater inter-class separation between and old and new classes.

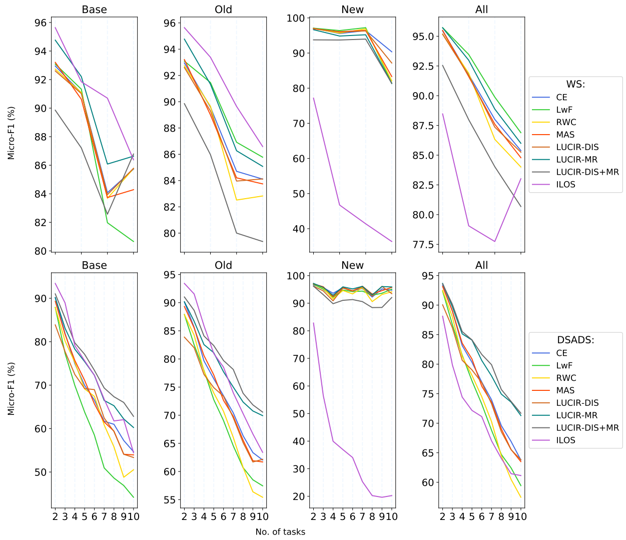

Figure 3. Accuracies detailed by base, old, new and all classes per incremental task.

Performance across base, new and old classes: While LUCIR-DIS+MR and LwF outperform other techniques on DSADS and WS respectively on overall tasks, an observation of the base, new and old class accuracies in Figure 3 offers additional insights into how different techniques respond to the *plasticity-stability* trade-off. ILOS, for instance, consistently performs poorer on new classes across both the data sets. However, the maximum scores of ILOS on base and old classes make it more robust to interferences due to new knowledge hence showing that even a direct tuning of the new model's logits based on the previous model can help surpass complex regularization operations. Together with this and the divergences between F1 macro and micro scores, we assume that ILOS's restrictiveness for new classes actually harms the learning when used in conjunction with MemR. We also observe that margin-ranking based methods (LUCIR-MR and LUCIR-DIS+MR) perform poorer than others on new tasks but are robust at preserving old knowledge. An intuitive explanation to this could be the design of MR that reinforces the model's confidence at recognizing ground truth embeddings for old class samples following multiple incremental training steps.

Varying holdout sizes: Drawing inspiration from the superior performance of replay-assisted learning, we further evaluate these for $S \in \{2, 4, 6, 8, 10, 15\}$. Figure 2 shows that even a small number of replay samples can yield a huge leap in the performance of the techniques than when ran without replay (Table 1). For WS, we see that the majority of the methods react in the same way to memory upgrades as their F1 scores start with a similar slope and reach a comparable pace starting from step 4. A few of them stick out: ILOS which mostly has a lower score than the rest but the slope is similar. LUCIR-DIS+MR reaches the level of most methods later and is less stable. We attribute these anomalies to the imbalanced sample distribution of WS. Looking at the results on DSADS which has perfectly balanced class distribution, this seems to be the case as we can see an almost linear increase in score with rising memory. Thus, we conclude that the working of regularization terms is more dependent on dataset characteristics than on the available memory.

5. Conclusion

In this paper, we have shown that the well known continuous learning regularization terms have no or only limited effect in human activity recognition scenarios when used with or without memory replay.

Memory replay, in particular, overshadows the value of regularization and some techniques even adversely affect the learning process. Most importantly, we advocate that the direction of continual learning research should not only focus vision tasks but also target other domains with diverse data distribution and resource constraints.

References

Afonso, L. C., Rosa, G. H., Pereira, C. R., Weber, S. A., Hook, C., Albuquerque, V. H. C., and Papa, J. P. A recurrence plot-based approach for Parkinson's disease identification. *Future Generation Computer Systems*, 2019. ISSN 0167739X. doi: 10.1016/j.future.2018.11.054.

Aljundi, R., Babiloni, F., Elhoseiny, M., Rohrbach, M., and Tuytelaars, T. Memory Aware Synapses: Learning What (not) to Forget. *ECCV*, 2018.

Altun, K. and Barshan, B. Human Activity Recognition Using Inertial/Magnetic Sensor Units. In *Proceedings of the First International Conference on Human Behavior Understanding*, HBU'10, pp. 38–51, Berlin, Heidelberg, 2010. Springer-Verlag. ISBN 3-642-14714-3, 978-3-642-14714-2. URL http://dl.acm.org/citation.cfm?id=1881331.1881338.

Chaudhry, A., Dokania, P. K., Ajanthan, T., and Torr, P. H. Riemannian Walk for Incremental Learning: Understanding Forgetting and Intransigence. In *Lecture Notes in Computer Science (including subseries Lecture Notes in Artificial Intelligence and Lecture Notes in Bioinformatics)*, 2018. ISBN 9783030012519. doi: 10.1007/978-3-030-01252-6_33.

Fang, L., Ye, J., and Dobson, S. Discovery and Recognition of Emerging Human Activities Using a Hierarchical Mixture of Directional Statistical Models. *IEEE Transactions on Knowledge and Data Engineering*, 32(7):1304–1316, jul 2020. ISSN 1041-4347. doi: 10.1109/TKDE.2019.2905207. URL https://ieeexplore.ieee.org/document/8667728/.

He, J., Mao, R., Shao, Z., and Zhu, F. Incremental Learning In Online Scenario. mar 2020. URL http://arxiv.org/abs/2003.13191.

Hinton, G., Vinyals, O., and Dean, J. Distilling the Knowledge in a Neural Network. mar 2015. URL http://arxiv.org/abs/1503.02531.

Hou, S., Pan, X., Loy, C. C., Wang, Z., and Lin, D. Learning a unified classifier incrementally via rebalancing. In *Proceedings of the IEEE Computer Society Conference on Computer Vision and Pattern Recognition*, 2019. ISBN 9781728132938. doi: 10.1109/CVPR.2019.00092.

Kemker, R., McClure, M., Abitino, A., Hayes, T. L., and Kanan, C. Measuring catastrophic forgetting in neural networks. In *Thirty-second AAAI conference on artificial intelligence*, 2018.

Kirkpatrick, J., Pascanu, R., Rabinowitz, N., Veness, J., Desjardins, G., Rusu, A. A., Milan, K., Quan, J., Ramalho, T., Grabska-Barwinska, A., Hassabis, D., Clopath, C., Kumaran, D., and Hadsell, R. Overcoming catastrophic forgetting in neural networks. dec 2016. URL http://arxiv.org/abs/1612.00796.

Li, Z. and Hoiem, D. Learning Without Forgetting. In *European Conference on Computer Vision 2016*, pp. 614–629. 2016. doi: 10.1007/978-3-319-46493-0_37. URL http://link.springer.com/10.1007/978-3-319-46493-0{_}37.

Liu, X., Masana, M., Herranz, L., Van De Weijer, J., Lopez, A. M., and Bagdanov, A. D. Rotate your Networks: Better Weight Consolidation and Less Catastrophic Forgetting. In *Proceedings - International Conference on Pattern Recognition*, 2018. ISBN 9781538637883. doi: 10.1109/ICPR.2018.8545895.

MacKay, D. J. C. A Practical Bayesian Framework for Backpropagation Networks. *Neural Computation*, 1992. ISSN 0899-7667. doi: 10.1162/neco.1992.4.3.448.

McCloskey, M. and Cohen, N. J. Catastrophic Interference in Connectionist Networks: The Sequential Learning Problem. *Psychology of Learning and Motivation - Advances in Research and Theory*, 1989. ISSN 00797421. doi: 10.1016/S0079-7421(08)60536-8.

Mermillod, M., Bugaiska, A., and Bonin, P. The stability-plasticity dilemma: investigating the continuum from catastrophic forgetting to age-limited learning effects. *Frontiers in Psychology*, 2013. ISSN 1664-1078. doi: 10.3389/fpsyg.2013.00504.

Wang, J., Chen, Y., Hu, L., Peng, X., and Yu, P. S. Stratified Transfer Learning for Cross-domain Activity Recognition. In *2018 IEEE International Conference on Pervasive Computing and Communications, PerCom 2018*, 2018. ISBN 9781538632246. doi: 10.1109/PERCOM.2018.8444572.

Ye, J., Dobson, S., and Zambonelli, F. Lifelong Learning in Sensor-Based Human Activity Recognition. *IEEE Pervasive Computing*, 2019. ISSN 15582590. doi: 10.1109/MPRV.2019.2913933.

Yoon, J., Kim, S., Yang, E., and Hwang, S. J. Scalable and Order-robust Continual Learning with Additive Parameter Decomposition. *arXiv e-prints*, art. arXiv:1902.09432, February 2019.

Zhang, Y., Tian, G., Zhang, S., and Li, C. A Knowledge-Based Approach for Multiagent Collaboration in Smart Home: From Activity Recognition to Guidance Service. *IEEE Transactions on Instrumentation and Measurement*, 2020. ISSN 15579662. doi: 10.1109/TIM.2019.2895931.

A. Loss Function Terms

LwF uses knowledge distillation loss to approximate the output of the original network:

$$\mathcal{L}_{KD}(y_o, \hat{y}_o) = -\sum_{i=1}^{l} y_o^{'(i)} \log \hat{y}_o^{'(i)}, \tag{1}$$

where l is the number of class labels, and $y_o^{'(i)}$ and $\hat{y}_o^{'(i)}$ are temperature-scaled *recorded* and *current* probabilities of the sample on a label l. The loss $\mathcal{L}_{KD}$ is combined with the cross-entropy loss on new task samples to form the *cross-distillation* loss:

$$\mathcal{L}(y_n, \hat{y}_n, y_o, \hat{y}_o) = \lambda o \mathcal{L}_{KD}(y_o, \hat{y}_o) + \mathcal{L}_{CE}(y_n, \hat{y}_n) \tag{2}$$

where λ_o is a loss balance weight computed as the ratio of old classes to total observed classes. A larger λ_o favors the old task performances over new task.

EWC assumes that if a dataset D consists of two independent tasks A and B, then the importance of parameters of the model is modeled as the posterior distribution $logp(\theta|D) = logp(D_B|\theta) + logp(\theta|D_A) - logp(D_B)$. $p(\theta|D_A)$ suggests which parameters are important to task A. The true posterior probability $p(\theta|D_A)$ is intractable, and thus it is estimated via Laplace approximation (MacKay, 1992) with precision determined by the Fisher Information Matrix (FIM). The loss function for EWC is defined as:

$$\mathcal{L}(\theta) = \mathcal{L}_B(\theta) + \sum_i \frac{\lambda}{2} F_i(\theta_i - \theta^*_{A,i})^2, \tag{3}$$

where $\mathcal{L}_B$ is the loss on task B, λ indicates the importance of the old task with respect to the new task, and i is the parameter index. **RWC** improves upon EWC by reparameterizing θ through rotation in a way that it does not change outputs of the forward pass but the FIM computed from gradients during the backward pass is approximately diagonal.

MAS considers approximating the importance of a network's parameters by learning the sensitivity of the objective function to a parameter change; *i.e.,* given a data point x_k whose network output is $F(x_k;\theta)$, a change in the network output caused by a small perturbation $\delta = \{\delta_{ij}\}$ in the parameters $\theta = \{\theta_{ij}\}$ can be approximated as: $F(x_k;\theta+\delta) - F(x_k;\theta) \approx \sum_{i,j} g_{ij}(x_k)\delta_{ij}$, where g is the gradient with respect to the parameter θ, and $g_{ij}(x_k) = \frac{\partial(F(x_k,\theta)}{\partial\theta_{ij}}$. Accumulating gradients over all the data points, the importance weight on a parameter θ_{ij} can be computed as: $\Omega_{ij} = \frac{1}{N}\sum_{k=1}^{N} ||g_{ij}(x_k)||$. While learning a new task, MAS then defines the loss function as:

$$\mathcal{L}(\theta) = \mathcal{L}_n(\theta) + \frac{\lambda}{2}\sum_{i,j}\Omega_{ij}(\theta_{ij} - \theta^*_{ij})^2, \tag{4}$$

where $\mathcal{L}_n(\theta)$ is the loss on the new task, θ_{ij} and θ^*_{ij} are the new and old network parameters, and λ is a hyperparameter that varies with the dataset.

LUCIR primarily targets the *class imbalance* arising due to a small amount of in-memory samples of old tasks and a large amount of samples of new tasks in the data of an incremental training step. This is tackled using two kinds of losses: (i) *less-forget constraint* loss ($\mathcal{L}^G_{dis}$) is introduced to preserve the spatial configuration of old classes' embeddings by encouraging the features extracted from the new model to be rotated in the direction similar to those of the old model, *i.e.,* $\mathcal{L}^G_{dis}(x) = 1 - \langle \tilde{f}^*(x), \tilde{f}(x)\rangle$, where $\tilde{f}(x)$ and $\tilde{f}^*(x)$ are normalised features extracted by the new and the old model respectively, and $\langle v_1, v_2\rangle$ denotes the cosine similarity between the vectors v_1 and v_2; (ii) *margin ranking* ($\mathcal{L}_{mr}$) loss is used to enhance inter-class separation by pushing the ground-truth old classes for each in-memory sample x far from all new classes it is confused with. To achieve this, the logits of ground-truth classes of x are treated *positive* while the logits of top-K classes that x is most confused with are treated as hard *negatives*, *i.e.,* $\mathcal{L}_{mr}(x) = \sum_{k=1}^{K} \max(m - \langle\tilde{\theta}(x), \tilde{f}(x)\rangle + \langle\tilde{\theta}^k . \tilde{f}(x)\rangle, 0)$. The loss function resulting from the combination of $\mathcal{L}^G_{dis}$ and $\mathcal{L}_{mr}$ can be given as:

$$L = \frac{1}{|N|}\sum_{x\in N}(L_{ce}(x) + \lambda L^G_{dis}(x)) + \frac{1}{|N_o|}\sum_{x\in N_o} L_{mr}(x), \tag{5}$$

where N is a training batch drawn from X and N_o represents the reserved old samples. λ is a hyperparameter that says how much knowledge of the previous model needs to be preserved depending on how many new classes are introduced and is computed by multiplying a fixed λ_{base} with the squared root of the fraction of new and old classes; *i.e.,* $\lambda = \lambda_{base}\sqrt{|C_N|/|C_o|}$.

ILOS uses an accommodation ratio $0 \leq \beta \leq 1$ to adjust the proportion of logits from the current model and the previous model:

$$\tilde{o_k} = \begin{cases} \beta o_k + (1-\beta)\hat{o_k} & 1 \leq k \leq n \\ o_k, & n+1 \leq k \leq n+m \end{cases} \tag{6}$$

where n is the number of classes observed till previous task, m is the number of classes in the current task, $\tilde{o_k}$ are the adjusted output logits and $\hat{o_k}$ are the output logits from the FC layer of the previous model. The adjusted norms of old classes are thus inclined either towards the range of norms of old classes of the current model or that of the previous model. The degree of this inclination is proportional to the magnitude of β. While $\mathcal{L}_{KD}$ in Equation 2 is still calculated using o_k, $\mathcal{L}_{CE}$ is now based on $\tilde{o_k}$ instead of o_k.

B. Inter-class Similarity

Figure 4 shows the correlation among raw features of activities in DSADS. Due to bodily restrictions and subject-specific fashion, different activities might have resemblance in distribution.

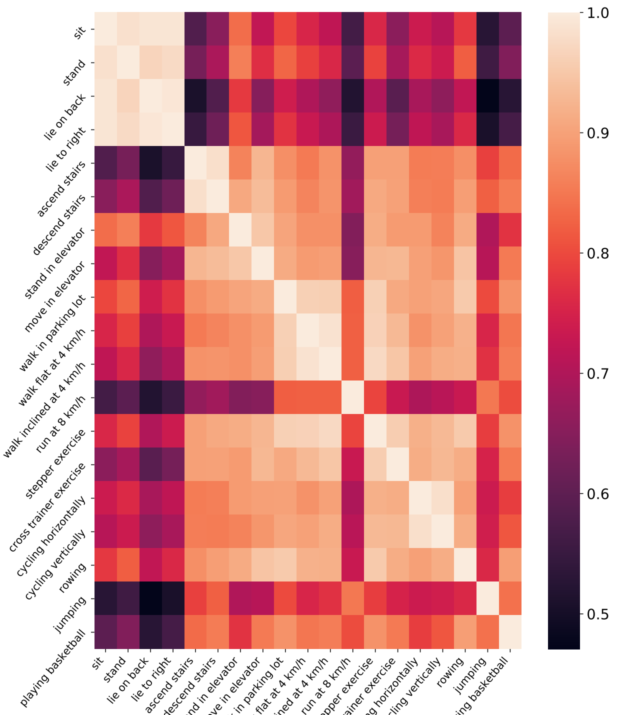

Figure 4. Correlation heatmap of activities in the DSADS accelerometer dataset.

C. Class distribution

As shown in Figure 5, the two datasets used in our work represent two different scenarios of class distribution apart from having captured using different sensor technologies.

D. Technique-specific hyperparameters

This is a brief overview over the hyperparameters derived by grid search. λ for LwF, RWC and MAS are set to 1.6, 3 and 0.25 each. LUCIR-based losses use a $\lambda_{base} = 5$, and m and k for LUCIR-MR are set to 0.5 and 2 each.

Table 2. Additional experiment hyperparameters

Dataset	WS	DSADS
Batch size	15	20
Initial Learning Rate	0.01	0.01
Epochs till Convergence	200	200
Learning Rate Scheduler Step Size (effective after)	40 (50)[4]	50 (50)
Weight Decay Rate	1.00E-04	1.00E-04

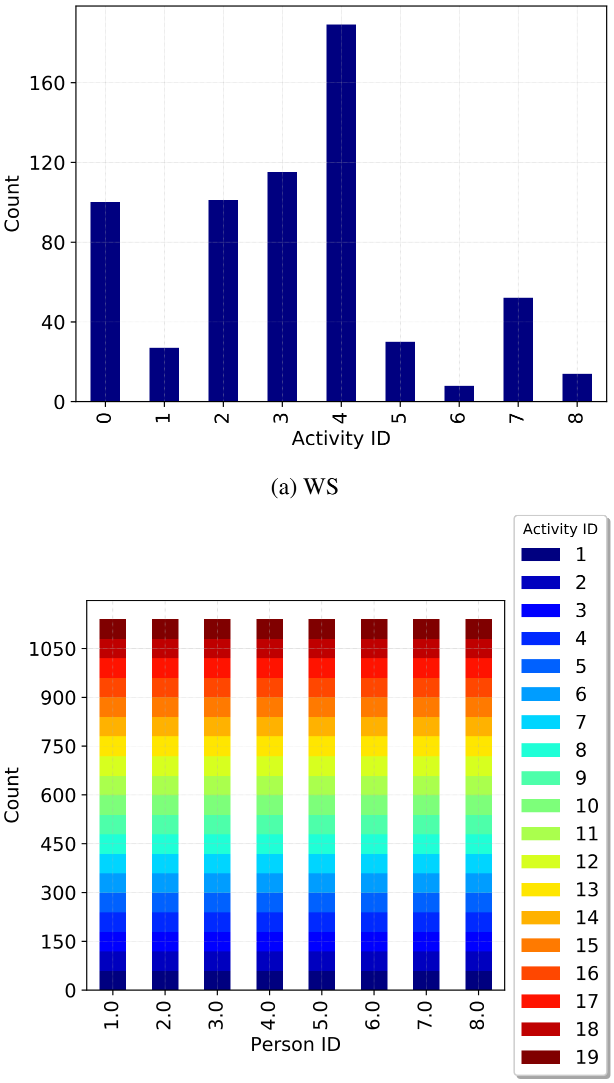

(a) WS

(b) DSADS

Figure 5. Frequency distribution of activities in WS and DSADS datasets.

E. Relative Divergence between F1 Micro and Macro Scores

Table 3. F1-Micro / F1-Macro in percent (%).

Method	WS Blank	WS Memory Replay	DSADS Blank	DSADS Memory Replay
CE	518.32	111.29	906.67	102.16
LwF	438.66	112.61	759.21	104.01
RWC	321.76	111.46	757.33	102.77
MAS	422.76	111.11	791.67	102.02
LUCIR-DIS	459.91	110.92	992.45	102.16
LUCIR-MR	-	111.51	-	101.77
LUCIR-DIS+MR	-	110.32	-	101.63
ILOS	253.05	113.54	477.78	102.89

[4] For example, learning rate for training on WS reduces by a factor of 0.01 after 90, 130 and 170 epochs.